Biometrics, 2024, 80(2), ujae036
https://doi.org/10.1093/biomtc/ujae036
Biometric Methodology

Testing conditional quantile independence with functional covariate

Yongzhen Feng[1], Jie Li[2,*], Xiaojun Song[3]

[1]Center for Statistical Science and Department of Industrial Engineering, Tsinghua University, Beijing 100084, China, [2]Center for Applied Statistics and School of Statistics, Renmin University of China, Beijing 100872, China, [3]Department of Business Statistics and Econometrics, Guanghua School of Management and Center for Statistical Science, Peking University, Beijing 100871, China

[*]Corresponding author: Jie Li, Center for Applied Statistics and School of Statistics, Renmin University of China, Beijing 100872, China (lijie_stat@ruc.edu.cn).

ABSTRACT

We propose a new non-parametric conditional independence test for a scalar response and a functional covariate over a continuum of quantile levels. We build a Cramer–von Mises type test statistic based on an empirical process indexed by random projections of the functional covariate, effectively avoiding the "curse of dimensionality" under the projected hypothesis, which is almost surely equivalent to the null hypothesis. The asymptotic null distribution of the proposed test statistic is obtained under some mild assumptions. The asymptotic global and local power properties of our test statistic are then investigated. We specifically demonstrate that the statistic is able to detect a broad class of local alternatives converging to the null at the parametric rate. Additionally, we recommend a simple multiplier bootstrap approach for estimating the critical values. The finite-sample performance of our statistic is examined through several Monte Carlo simulation experiments. Finally, an analysis of an EEG data set is used to show the utility and versatility of our proposed test statistic.

KEYWORDS: empirical process; functional data; multiplier bootstrap; quantile independence; random projections.

1 INTRODUCTION

As digital technology develops significantly, there are more and more instances from the biosciences where the obtained data are curves. An exciting example is the electroencephalogram (EEG) data for a person in a resting state with eyes closed. The participant went through a 5-min test, and EEG signals were recorded at a sampling rate of 1000 Hz. Since the densely recorded EEG signals have few measurement errors, they can be naturally regarded as functional data. Functional data analysis views data as realizations of random functions and takes into account the functional nature of the data. Over the past 2 decades, it has become an important area of statistics, extending the analysis of multivariate data to more complicated and informative curve data, see Silverman and Ramsay (2002), Ramsay and Silverman (2005), Ferraty and Vieu (2006), and Hsing and Eubank (2015) for basic theory and applications.

Many studies have suggested that human intelligence or cognitive function may be related to EEG, see Zhang et al. (2020). A practically important issue lies in investigating the relationship between working memory ability and EEG. Introduced by Koenker and Bassett (1978), quantile regression models the distributional relationship between a set of covariates and specific quantiles of interest of a target response. Due to its robustness against outliers in response measurements, it finds extensive use in biosciences and other scientific disciplines. More importantly, as it enables the description of the influence of covariates on the complete conditional distribution of the response, quantile regression is particularly helpful when conditional quantile functions are of interest.

Combining quantile regression with functional data leads to functional quantile regression, in which the most popular is functional linear quantile regression. It has been extensively investigated; for a comprehensive treatment in estimation and inference of functional linear quantile regression models (FLQMs), see Cardot et al. (2005), Chen and Müller (2012), and Kato (2012). Additionally, non-parametric quantile regression has been extended to functional data, as in Chowdhury and Chaudhuri (2019). The majority of the aforementioned papers concentrate on utilizing either linear models or non-parametric models to describe the conditional quantile of the response variable given the functional covariate. Determining whether the functional covariate $\mathbf{X}$, taking values in a Hilbert space $\mathcal{H}$, actually contributes to the conditional quantiles of an $\mathbb{R}$-valued random variable Y for the interested quantile levels, however, is a more fundamental question and the first step in conditional quantile modeling. The formal null hypothesis for this problem is as follows:

$$H_0 : \mathbb{P}\left\{Y \le Q_Y(\tau)|\mathbf{X}\right\} = \tau \ \text{ almost surely } \ (a.s.) \quad \text{for all } \tau \in \mathcal{A}, \tag{1}$$

where $Q_Y(\tau)$ is the unconditional quantile of Y at quantile level τ, which is defined as $Q_Y(\tau) = \inf\left\{y : F(y) \ge \tau\right\}$ with $F(\cdot)$ the cumulative distribution function (CDF) of Y, and $\mathcal{A}$ is a

Received: September 16, 2023; Revised: March 10, 2024; Accepted: April 25, 2024

compact subinterval of $(0, 1)$, which collects the quantile levels of interest. If H_0 is supported by the data, there is no need to pursue a quantile regression model for Y given the functional covariate $\mathbf{X}$ at any quantile $\tau \in \mathcal{A}$, which drastically reduces the statistical modeling of Y.

It is important to note that our test for Equation 1 is quite general. When the set $\mathcal{A}$ is fairly close to the whole interval $(0, 1)$, say $\mathcal{A} = [\epsilon, 1 - \epsilon]$ for some arbitrarily small $\epsilon > 0$, it becomes the conditional distribution independence test of Y given $\mathbf{X}$; namely, testing the statistical independence of Y and $\mathbf{X}$: $F_{Y|\mathbf{X}}(\cdot) = F(\cdot)$, where $F_{Y|\mathbf{X}}(\cdot)$ denotes the conditional distribution function of Y given $\mathbf{X}$. Our test also includes testing conditional mean independence for functional data, that is, $\mathbb{E}(Y|\mathbf{X}) = \mathbb{E}(Y)$, as a special case. Indeed, although the mean does not depend on $\mathbf{X}$, other regions of the distribution of Y may be dependent on $\mathbf{X}$. As a result, our test can detect both mean and distributional relationships between Y and $\mathbf{X}$. In particular, our test may be able to identify the regions of dependence by varying $\mathcal{A}$ properly. On the other hand, the proposed test reduces to checking the conditional quantile independence at a single quantile when $\mathcal{A}$ only contains a single quantile level in $(0, 1)$.

To our knowledge, there is currently no study investigating the conditional quantile independence of Y given a functional covariate $\mathbf{X}$ over a continuum of quantile levels, as described by the null hypothesis in Equation 1. Lee et al. (2020) utilized functional martingale difference divergence to perform the conditional mean independence test for a response variable and a predictor variable where either or both can be function-valued. Their proposed test only focused on the conditional mean independence test and omitted the quantile scenario, thus limiting the scope of their suggested test. Escanciano and Goh (2014) introduced a non-parametric test for the correct specification of a linear conditional quantile function over a continuum of quantiles. However, they did not take functional-valued covariates into account and instead assumed the covariates to be a d-dimensional random vector. Finally, Shi et al. (2021) proposed a non-parametric U-process test statistic based on the functional principal component analysis to check the adequacy of the FLQM. However, their test was constructed at a single specific quantile rather than employing a continuum of quantile levels.

In our paper, we characterize the null hypothesis 1 via a projected hypothesis and propose an empirical process indexed by random projections of the functional covariate, that is, the inner product of the functional variable $\mathbf{X}$ and an appropriate projection direction $\mathbf{h} \in \mathcal{H}$. The proposed test statistic is then constructed as a Cramer–von Mises norm of the resulting empirical process, whose limiting null distribution is established under some mild assumptions. We also investigate its asymptotic behavior under the fixed alternative and a certain sequence of local alternatives approaching the null at the parametric rate.

The main contribution of this work is as follows. First, we employ random projection of the functional covariate to circumvent the curse of dimensionality. Unlike the local smoothing-based tests, which rely on user-chosen tuning parameters such as bandwidth and can only detect local alternatives converging to the null at a slower convergence rate that depends on the tuning parameter, our test is built upon a marked empirical process indexed by a random projection of the functional covariate as introduced in Cuesta-Albertos et al. (2019) and is able to detect local alternatives at the fastest parametric rate. As a result, our test is robust and powerful in a variety of situations. We select several different projection directions based on a data-driven approach to reduce the impact of projection direction $\mathbf{h}$ on the testing results. To achieve higher accuracy in both size and power performance, the final P-value of the test is obtained by merging the series of P-values under different projection directions using the false discovery rate (FDR) method in Benjamini and Yekutieli (2001). Second, a multiplier bootstrap is used to compute critical values of the limiting null distribution. The computational efficiency is remarkably increased since, unlike the widely used wild bootstrap method, there is no need to reestimate the parameter at each bootstrap replication for the multiplier bootstrap. It is important to note that the traditional residual-based wild bootstrap procedure fails to be valid under the framework of a continuum of quantiles since its resampling procedure can only be implemented at a single quantile, making it unable to mimic the original data structure. We demonstrate that the multiplier bootstrap has good theoretical properties, such as bootstrap consistency under the null hypothesis, in addition to being simple to apply. Third, the proposed test is flexible enough to measure the quantile independence at the whole quantile interval, a single point, or any interior intervals. It offers a trustworthy inferential tool to comprehensively evaluate the independence with functional covariates. Monte Carlo simulation findings indicate that these appealing features translate to tests with excellent finite sample performance, which also strongly corroborates the asymptotic theory.

The rest of the paper is organized as follows. In Section 2, we present the testing framework and introduce our proposed test statistic based on hypothesis projection. We establish the asymptotic properties of the proposed test under mild assumptions in Section 3. Procedures to implement the proposed test are reported in Section 4 with details. Then we examine the finite sample performance of our test via Monte Carlo simulations in Section 5. This is followed by an analysis of the EEG data set in Section 6. Finally, Section 7 concludes the paper. Additional simulation results and all technical proofs can be found in Supplementary Materials.

Throughout this paper, $\mathcal{H}$ is a separable Hilbert space endowed with the inner product $\langle \cdot, \cdot \rangle$ and associated norm $\|\cdot\|_{\mathcal{H}}$, and $\mathbf{X}$ is a $\mathcal{H}$-valued r.v. defined on (Ω, σ, ν). For any $\mathbf{X} \in \mathcal{H}$, denote its norm $\|\mathbf{X}\|_{\mathcal{H}} = \langle \mathbf{X}, \mathbf{X} \rangle^{1/2}$. Given $\mathbf{h} \in \mathcal{H}$, denote by $\mathbf{X}^{\mathbf{h}} = \langle \mathbf{X}, \mathbf{h} \rangle$ the projected $\mathbf{X}$ on the direction $\mathbf{h}$. The indicator of an event A is denoted by $I(A)$, that is, $I(A) = 1$ if A occurs, and zero otherwise. Weak convergence is denoted by $\overset{\mathcal{L}}{\rightsquigarrow}$ and $a_n \sim b_n$ means $a_n / b_n \to 1$, as $n \to \infty$.

2 TESTING PROCEDURE

We now introduce a marked empirical process indexed by random projections of the functional covariate to construct the aforementioned test. The null hypothesis 1 can be re-expressed as $H_0 : \mathbb{E}\left[I\left\{Y \leq Q_Y(\tau)\right\} - \tau | \mathbf{X}\right] = 0$ *a.s.* for all $\tau \in \mathcal{A}$, which can also be characterized using the associated pro-

jected hypothesis on a randomly chosen $\mathbf{h} \in \mathcal{H}$, defined as

$$H_{0,\mathbf{h}} : \mathbb{E}\left[I\left\{Y \leq Q_Y(\tau)\right\} - \tau | \mathbf{X}^{\mathbf{h}}\right] = 0 \ \ a.s. \ \text{ for all } \tau \in \mathcal{A}. \tag{2}$$

The following lemma specifies formally the necessary and sufficient condition such that $\mathbb{E}\left[I\left\{Y \leq Q_Y(\tau)\right\} - \tau | \mathbf{X}^{\mathbf{h}}\right] = 0$ *a.s.* holds based on projections of $\mathbf{X}$.

Lemma 1 *(Theorem 2.4, Cuesta-Albertos et al. (2019)) Let μ be a non-degenerate Gaussian measure on $\mathcal{H}$. Denote $\mathcal{H}_0 := \left\{\mathbf{h} \in \mathcal{H} : \mathbb{E}\left[I\left\{Y \leq Q_Y(\tau)\right\} - \tau | \mathbf{X}^{\mathbf{h}}\right] = 0 \ a.s.\right\}$, under Assumption (A1) in Section 3, there exists*

$$\mathbb{E}\left[I\left\{Y \leq Q_Y(\tau)\right\} - \tau | \mathbf{X}\right] = 0 \ a.s. \iff \mu(\mathcal{H}_0) > 0.$$

The above lemma establishes the μ-*a.s.* equivalence between the original null hypothesis H_0 and the projected version $H_{0,\mathbf{h}}$. Specifically, if H_0 holds, then the law of iterated expectation ensures $H_{0,\mathbf{h}}$ holds for every $\mathbf{h} \in \mathcal{H}$. If H_0 fails, Lemma 1 entails that the set of projections for which H_0 is not congruent with $H_{0,\mathbf{h}}$ has measure zero, that is, $\mu(\mathcal{H}_0) = 0$, implying that with probability 1, one can choose a projection $\mathbf{h}$ such that $H_{0,\mathbf{h}}$ fails. Thus, to test the null hypothesis H_0, one just first chooses a random projected direction $\mathbf{h} \in \mathcal{H}$, and then tests the projected null hypothesis $H_{0,\mathbf{h}}$ in Equation 2. However, sometimes the power of the resulting test may be sensitive to the selected projection. To lower the influence of the projection direction and improve power performance, we recommend choosing several different directions. A detailed selection procedure for the projection directions is discussed in Section 4.

Chosen a random projection $\mathbf{h}$ in $\mathcal{H}$, the projected null hypothesis in Equation 2 can be rewritten as $\mathbb{E}\left[\psi_\tau\left\{Y, Q_Y(\tau)\right\} | \mathbf{X}^{\mathbf{h}}\right] = 0$, where

$$\psi_\tau(y, q) = I\left\{y \leq q\right\} - \tau, \quad \text{for } q, y \in \mathbb{R}.$$

To estimate $\psi_\tau\{Y, Q_Y(\tau)\}$, instead of using the direct plugging-in estimator, we consider smoothing the indicator function $I\{Y \leq Q_Y(\tau)\}$ to simplify the derivation of the theoretical results. Let $K(u) = \int_{-\infty}^{u} k(\bar{u})d\bar{u}$, with $k(u) \equiv dK(u)/du$ a user-chosen univariate non-negative symmetric kernel function that integrates to 1, for example, a standard normal PDF. In addition, let $a = a_n \in \mathbb{R}^+$ be a positive sequence of bandwidth parameters shrinking to zero at a proper rate as $n \to \infty$. Given the data set $\left\{(\mathbf{X}_i, Y_i)\right\}_{i=1}^n$, we propose the test process as

$$T_{n,\mathbf{h}}(x, \tau) = \frac{1}{\sqrt{n}} \sum_{i=1}^{n} \psi_{\tau,a}\left\{Y_i, \widehat{Q}_Y(\tau)\right\} I\left(\mathbf{X}_i^{\mathbf{h}} \leq x\right), \tag{3}$$

where

$$\psi_{\tau,a}(y, q) = K\left\{\frac{q - y}{a}\right\} - \tau, \quad \text{for } q, y \in \mathbb{R},$$

and $\widehat{Q}_Y(\tau) = \arg\min_q \sum_{i=1}^n \rho_\tau(Y_i - q)$, with $\rho_\tau(u) = u\{\tau - I(u < 0)\}$ being the quantile loss function. Note that when $a = 0$, $K\{(\cdot - Y)/a\}$ essentially reduces to the indicator function $I(Y \leq \cdot)$. It is shown in Web Appendix B of the Supplementary Materials that $\psi_{\tau,a}\left\{Y, \widehat{Q}_Y(\tau)\right\}$ facilitates the investigation of the estimation effect caused by $\widehat{Q}_Y(\tau)$.

The test statistic is proper continuous functionals of $T_{n,\mathbf{h}}$. In our paper, we focus on the popular Cramer–von Mises (CvM) norm to measure the distance of $T_{n,\mathbf{h}}$ from zero. The CvM norm is given by

$$\|T_{n,\mathbf{h}}\|_{CvM} := \int_{\mathbb{R}\times\mathcal{A}} T_{n,\mathbf{h}}^2(x, \tau)\, dF_{n,\mathbf{h}}(x)d\tau,$$

where $F_{n,\boldsymbol{h}}(x) = n^{-1}\sum_{i=1}^n \mathbb{1}_{\{\mathbf{X}_i^{\mathbf{h}} \leq x\}}$ is the empirical distribution function based on the randomly projected functional covariate $\{\mathbf{X}_i^{\mathbf{h}}\}_{i=1}^n$. Note that this norm does not admit a closed form; thus, we use Monte Carlo integration to approximate it, with the corresponding test statistic CvM_n defined as

$$\text{CvM}_n = \frac{1}{mn} \sum_{j=1}^{m} \sum_{i=1}^{n} \left|T_{n,\mathbf{h}}\left(\mathbf{X}_i^{\mathbf{h}}, \alpha_j\right)\right|^2, \tag{4}$$

where $\{\alpha_j\}_{j=1}^m$ are dense regular grids in $\mathcal{A}$ with $m \to \infty$ as $n \to \infty$. The null hypothesis H_0 is rejected whenever the test statistic CvM_n exceeds some "large" values, which are consistently estimated using a multiplier bootstrap procedure, as described in Section 3.3.

Remark 1 *In this paper, we have focused on the projected hypothesis with 1 random projection. However, it is possible to extend the test based on multiple random projections. After selecting a set of projections $\left\{\mathbf{h}_j\right\}_{j=1}^{n.proj}$, we can obtain the corresponding testing processes $\left\{T_{n,\mathbf{h}_j}\right\}_{j=1}^{n.proj}$ respectively as in Equation 3, and build a vector testing process $\left(T_{n,\mathbf{h}_1}, \ldots, T_{n,\mathbf{h}_{n.proj}}\right)^\top$. The CvM-type test statistic should also be modified accordingly. But this is not an easy task, owing to the elusive theory of the multidimensional projected hypothesis compared with 1-dimensional ones. Details of this extension are left for future research.*

3 ASYMPTOTIC RESULTS

In this section, we construct the limiting distribution of the empirical process $T_{n,\mathbf{h}}$ given in Equation 3 under both the null hypothesis and different types of alternatives. In addition, we also construct the consistency of a multiplier bootstrap approximation of the asymptotic null distribution. We first introduce some technical assumptions.

(A1) $\left\{(\mathbf{X}_i, Y_i)\right\}_{i=1}^n$ is a sequence of i.i.d. random variates with $\mathbb{E}\|\mathbf{X}\|_{\mathcal{H}}^2 < \infty$ and $\mathbb{E}|Y|^\beta < \infty$, for some $\beta \geq 2$. Moreover, $\sum_{k=1}^{\infty} m_k^{-1/k} = \infty$ with $m_k := \int \|\mathbf{X}\|_{\mathcal{H}}^k \, d\nu < \infty$ for all $k \geq 1$.

(A2) $f(\cdot)$, the Lebesgue density function of $F(\cdot)$, satisfies $\inf_{\tau\in\mathcal{A}} f\left\{Q_Y(\tau)\right\} > 0$. Its second-order derivative $f'(\cdot)$ is uniformly bounded from above on $\mathbb{R}$ *a.s.*.

(A3) The conditional CDF of Y given $\mathbf{X}$ projected in any direction $\mathbf{h} \in \mathcal{H}$, $F(\cdot | \mathbf{X}^{\mathbf{h}})$, has up to qth order continuous derivatives, which are denoted, respectively, by $F^{(s)}\left(\cdot | \mathbf{X}^{\mathbf{h}}\right)$, $s = 1, 2, \cdots, q$, for $q \geq 2$, with $F^{(q)}(\cdot | \mathbf{X}^{\mathbf{h}})$ uniformly bounded from above and continuous on $\mathbb{R}$ *a.s.*. Its Lebesgue density function $f(\cdot | \mathbf{X}^{\mathbf{h}})$ satisfies $\inf_{\tau\in\mathcal{A}} f\left\{Q_Y(\tau) | \mathbf{X}^{\mathbf{h}}\right\} \geq l_1 > 0$ *a.s.* and $\inf_{\tau\in\mathcal{A}} f\left\{Q_Y\left(\tau, \mathbf{X}^{\mathbf{h}}\right) | \mathbf{X}^{\mathbf{h}}\right\} \geq l_2 > 0$

a.s. for some constants l_1, l_2, where $Q_Y(\tau, \mathbf{X^h}) = \inf\{y : F(y|\mathbf{X^h}) \geq \tau\}$.

(A4) $Q_Y(\tau)$ is uniformly bounded and Lipschitz continuous for $\tau \in \mathcal{A}$ and $Q_Y(\tau, x)$ is uniformly bounded and Lipschitz continuous for $(\tau, x) \in \mathcal{A} \times \mathbb{R}$.

(A5) $K(\cdot)$ is first-time differentiable satisfying $\lim_{u \to -\infty} K(u) = 0$, $\lim_{u \to \infty} K(u) = 1$. $K(\cdot)$ and its first-order derivative $K'(\cdot)$ are uniformly bounded on $\mathbb{R}$ *a.s.*. $K'(\cdot)$ is symmetric over its support. There exists $P \geq 2$ such that $\int_{-\infty}^{\infty} u^s K'(u)du = \delta_{s0}$, for $s = 0, 1, \cdots, p-1$ and $\int_{-\infty}^{\infty} u^p K'(u)du < \infty$, where δ_{s0} is Kronecker's delta.

(A6) $na^{2q} \to 0$ and $na^2 \to \infty$, as $n \to \infty$, $a \to 0$.

Remark 2 *The first 2 assumptions are quite common. It is worth noting that the condition on m_k in (A1) can be easily satisfied. As Cuesta-Albertos et al. (2019) pointed out, this condition holds if the tails of $P_{\mathbf{X}}$, the law of $\mathbf{X}$, are light enough or if $\mathbf{X}$ has a finite moment generating function in a neighborhood of zero, thus the most commonly used Gaussian process is included. The moment condition of Y and the collective boundedness of $f(\cdot)$ and $f'(\cdot)$ are imposed to apply the uniform Bahadur representation as in Lemma B.3. Assumptions (A3) and (A4) assign the smoothness restriction to $F(\cdot|\mathbf{X^h})$ and $Q_Y(\cdot)$ for the application of empirical process theory. Assumptions (A5) and (A6) concern about CDF-version kernel $K(\cdot)$ and its related bandwidth a. If $q = 2$, the CDF of the standard normal meets all the conditions on $K(\cdot)$, one can choose $a \sim n^{-1/3}$. If $q = 4$, one can use the integral of the fourth-order Gaussian or Epanechnikov kernel as $K(\cdot)$ with $a \sim n^{-1/5}$.*

3.1 Asymptotic null distribution

Define an auxiliary process

$$S_{n0,\mathbf{h}}(x, \tau) = \frac{1}{\sqrt{n}} \sum_{i=1}^{n} \psi_\tau \{Y_i, Q_Y(\tau)\} \times \{I(\mathbf{X}_i^{\mathbf{h}} \leq x) - F_{\mathbf{h}}(x)\}, \quad (5)$$

where $F_{\mathbf{h}}(x) = \mathbb{E}\{I(\mathbf{X}^{\mathbf{h}} \leq x)\}$, namely the distribution function of $\mathbf{X}^{\mathbf{h}}$. The above process facilitates the construction of a multiplier bootstrap statistic in Section 3.3.

We show the asymptotic uniform equivalence between $T_{n,\mathbf{h}}$ and $S_{n0,\mathbf{h}}$ in Theorem 1. Then, we study the weak convergence of $S_{n0,\mathbf{h}}$ and obtain the asymptotic null distribution of $T_{n,\mathbf{h}}$ in Theorem 2.

Theorem 1 *Under $H_{0,\boldsymbol{h}}$ and Assumptions (A1)–(A6),*

$$\sup_{(x,\tau) \in \mathbb{R} \times \mathcal{A}} \left| T_{n,\mathbf{h}}(x, \tau) - S_{n0,\mathbf{h}}(x, \tau) \right| = o_{\mathbb{P}}(1).$$

Remark 3 *It is worth noting that*

$$T^{\#}_{n,\mathbf{h}}(x, \tau) = \frac{1}{\sqrt{n}} \sum_{i=1}^{n} \psi_{\tau,a} \{Y_i, \widehat{Q}_Y(\tau)\} \times \{I(\mathbf{X}_i^{\mathbf{h}} \leq x) - \widehat{F}_{\mathbf{h}}(x)\}, \quad (6)$$

with $\widehat{F}_{\mathbf{h}}(x) = n^{-1} \sum_{j=1}^{n} I(\mathbf{X}_j^{\mathbf{h}} \leq x)$ is also a feasible test process for Equation 2. It is simply the sample analogue of $S_{n0,\boldsymbol{h}}$, enjoying the same asymptotic expansion under $H_{0,\boldsymbol{h}}$ as the test process $T_{n,\boldsymbol{h}}$ given in Equation 3. By applying similar arguments in the proof of Theorem 1 in Web Appendix B in Supplementary Materials with $I(\boldsymbol{X^h} \leq x)$ replaced by 1, we can obtain that the difference between $T^{\#}_{n,\mathbf{h}}$ and $T_{n,\boldsymbol{h}}$ is asymptotically negligible. In our paper, we examine the finite-sample performance of $T^{\#}_{n,\mathbf{h}}$ while omitting its asymptotic properties to avoid repetition.

Theorem 2 *Under $H_{0,\boldsymbol{h}}$ and Assumptions (A1)–(A6),*

$$T_{n,\mathbf{h}} \overset{\mathcal{L}}{\rightsquigarrow} \mathcal{G},$$

where $\mathcal{G}$ is a Gaussian process with mean zero and covariance function $K(x_1, x_2, \tau_1, \tau_2) = (\min\{\tau_1, \tau_2\} - \tau_1\tau_2)[F_{\boldsymbol{h}}(\min\{x_1, x_2\}) - F_{\boldsymbol{h}}(x_1)F_{\boldsymbol{h}}(x_2)]$.

Continuous mapping theorem and Theorem 2 entail the asymptotic null distribution of CvM_n in the following corollary.

Corollary 1 *Under $H_{0,\boldsymbol{h}}$ and Assumptions (A1)–(A6),*

$$CvM_n \overset{\mathcal{L}}{\rightsquigarrow} \int_{\mathbb{R} \times \mathcal{A}} \mathcal{G}^2(x, \tau) dF_{\mathbf{h}}(x) d\tau.$$

The null hypothesis is rejected whenever CvM_n exceeds some overly "large" values. However, the above corollary has shown that the resulting asymptotic null distribution of CvM_n, that is, $\int_{\mathbb{R} \times \mathcal{A}} \mathcal{G}^2(x, \tau) dF_{\mathbf{h}}(x) d\tau$, depends on the underlying data-generating process in a complicated manner. Thus, the asymptotic critical values for CvM_n cannot be tabulated. To tackle this issue, we adopt an easy-to-implement multiplier bootstrap procedure to simulate the critical values of $\int_{\mathbb{R} \times \mathcal{A}} \mathcal{G}^2(x, \tau) dF_{\mathbf{h}}(x) d\tau$ as accurately as desired, with details given in Section 3.3.

3.2 Asymptotic power

In what follows, we investigate the asymptotic power properties of $T_{n,\mathbf{h}}$ under the fixed (ie, global) alternative, as well as a certain sequence of local alternatives converging to the null at the parametric rate. We first consider the fixed alternative hypothesis of the type

$$H_1 : \mathbb{E}\{\psi_\tau \{Y, Q_Y(\tau)\} | \mathbf{X}\} \neq 0 \ a.s., \quad \text{for some } \tau \in \mathcal{A}, \quad (7)$$

with the corresponding projected version

$$H_{1,\mathbf{h}} : \mathbb{E}\{\psi_\tau \{Y, Q_Y(\tau)\} | \mathbf{X^h}\} \neq 0 \ a.s., \quad \text{for some } \tau \in \mathcal{A}. \quad (8)$$

Note that $H_{1,\mathbf{h}}$ is simply the negation of $H_{0,\mathbf{h}}$. The following theorem states the asymptotic distribution of $T_{n,\mathbf{h}}$ under $H_{1,\mathbf{h}}$.

Theorem 3 *Under $H_{1,\boldsymbol{h}}$ and Assumptions (A1)–(A6),*

$$\sup_{(x,\tau) \in \mathbb{R} \times \mathcal{A}} \left| n^{-1/2} T_{n,\mathbf{h}}(x, \tau) - \mathcal{G}_1(x, \tau) \right| = o_{\mathbb{P}}(1),$$

where $\mathcal{G}_1(x, \tau) = \mathbb{E}[f\{Q_Y(\tau, \mathbf{X^h})|\mathbf{X^h}\}\{Q_Y(\tau) - Q_Y(\tau, \mathbf{X^h})\} I(\mathbf{X^h} \leq x)]$.

It is easy to see from Theorem 3 that under the fixed alternative $H_{1,\mathbf{h}}$, $\mathcal{G}_1(x,\tau) \neq 0$ for at least some τ and x with a positive measure. Therefore, $T_{n,\mathbf{h}}$ diverges and the test statistic CvM_n diverges to positive infinity at the rate of n, implying that our test is consistent against the fixed projected alternative $H_{1,\mathbf{h}}$ and thus is consistent against H_1.

Next, we study the asymptotic distribution of $T_{n,\mathbf{h}}$ under a sequence of local alternative hypotheses converging to the null at the parametric rate $n^{-1/2}$ given by

$$H_{1n}: \mathbb{E}\left[\psi_\tau\left\{Y, Q_Y(\tau)\right\}|\mathbf{X}\right] = n^{-1/2}\delta(\tau,\mathbf{X}) + \delta_n^R(\tau,\mathbf{X}) \ \ a.s., \quad \text{for all } \tau \in \mathcal{A}, \tag{9}$$

with the corresponding projected version

$$H_{1n,\mathbf{h}}: \mathbb{E}\left[\psi_\tau\left\{Y, Q_Y(\tau)\right\}|\mathbf{X}^{\mathbf{h}}\right] = n^{-1/2}\mathbb{E}\left\{\delta(\tau,\mathbf{X})\left|\mathbf{X}^{\mathbf{h}}\right.\right\} + \mathbb{E}\left\{\delta_n^R(\tau,\mathbf{X})\left|\mathbf{X}^{\mathbf{h}}\right.\right\} \ \ a.s., \quad \text{for all } \tau \in \mathcal{A}. \tag{10}$$

We require the functions $\delta(\tau,\mathbf{X})$ and $\delta_n^R(\tau,\mathbf{X})$ to satisfy the following assumption:

(A7) $\delta(\cdot,\mathbf{X})$ is continuous in $\mathcal{A}$ a.s., $\mathbb{E}\left\{\sup_{\tau\in\mathcal{A}}\left|\delta(\tau,\mathbf{X})\right|\right\} < \infty$ and $\mathbb{E}\left\{\sqrt{n}\sup_{\tau\in\mathcal{A}}\left|\delta_n^R(\tau,\mathbf{X})\right|\right\} = o(1)$.

Note that $n^{-1/2}$ signifies the rate of $H_{1n,\mathbf{h}}$ converging to $H_{0,\mathbf{h}}$ as n increases, which is known as the fastest rate possible for specification tests to be able to non-trivially detect local alternatives. The following theorem states the asymptotic distribution of $T_{n,\mathbf{h}}$ under the sequence of local alternatives $H_{1n,\mathbf{h}}$.

Theorem 4 *Under $H_{1n,\mathbf{h}}$ and Assumptions (A1)–(A7),*

$$T_{n,\mathbf{h}} \overset{\mathcal{L}}{\rightsquigarrow} \mathcal{G} + \Delta,$$

where $\mathcal{G}$ is the Gaussian process defined in Theorem 2, and Δ is a deterministic shift function given by

$$\Delta(x,\tau) = -\mathbb{E}\left[\delta(\tau,\mathbf{X})\left\{I\left(\mathbf{X}^{\mathbf{h}} \le x\right) - F_{\mathbf{h}}(x)\right\}\right].$$

Theorem 4 and the continuous mapping theorem lead to that, under $H_{1n,\mathbf{h}}$,

$$CvM_n \overset{\mathcal{L}}{\rightsquigarrow} \int_{\mathbb{R}}\left\{\mathcal{G}(x,\tau) + \Delta(x,\tau)\right\}^2 dF_{\mathbf{h}}(x)d\tau.$$

Therefore, our test has non-negligible asymptotic powers against the sequence of local alternatives $H_{1n,\mathbf{h}}$ since the shift function $\Delta(x,\tau) \neq 0$ for at least some x and τ with a positive measure.

3.3 Multiplier bootstrap approximation

It is shown in Theorem 2 that the limiting null distribution of $T_{n,\mathbf{h}}$ is non-pivotal, depending on the unknown distribution function $F_{\mathbf{h}}(\cdot)$. We suggest an easy-to-implement multiplier bootstrap method to approximate the limiting null distribution. Multiplier bootstrap, based on the multiplier central limit theorem in Section 2.9 of Vaart and Wellner (1996), has been widely applied to approximate Gaussian processes so as to obtain valid critical values, see Chernozhukov et al. (2013), Bücher and Kojadinovic (2016), Lemyre and Quessy (2017), Sant'Anna and Song (2019), and Chen and Zhou (2020). The key idea of multiplier bootstrap is to multiply the asymptotic analytic expression of the limiting process with mean zero and unit variance pseudo-random variables that are independent of the sample path, thus capable of maintaining the first and second moments of the original process and achieving a good approximation.

In our paper, the proposed multiplier bootstrap test process is

$$T_{n,\mathbf{h}}^*(x,\tau) = \frac{1}{\sqrt{n}}\sum_{i=1}^n \psi_{\tau,a}\left\{Y_i, \widehat{Q}_Y(\tau)\right\} \times \left\{I\left(\mathbf{X}_i^{\mathbf{h}} \le x\right) - \widehat{F}_{\mathbf{h}}(x)\right\} V_i, \tag{11}$$

where $\{V_i\}_{i=1}^n$ is a sequence of i.i.d. multiplier variables with mean 0 and variance 1 and independent of $\left\{(\mathbf{X}_i, Y_i)\right\}_{i=1}^n$. A classical choice of $\{V_i\}_{i=1}^n$ is $\mathbb{P}(V_i = 1-\kappa) = \kappa/\sqrt{5}$, $\mathbb{P}(V_i = \kappa) = 1 - \kappa/\sqrt{5}$, where $\kappa = \left(\sqrt{5}+1\right)/2$, as suggested in Mammen (1993). Note that the bootstrap test process Equation 11 depends on the original sample $\left\{(\mathbf{X}_i, Y_i)\right\}_{i=1}^n$. Denote "$\overset{\mathcal{L}^*}{\rightsquigarrow}$ in probability" the weak convergence in probability under the bootstrap law, that is, conditional on the original sample $\left\{(\mathbf{X}_i, Y_i)\right\}_{i=1}^n$. The following theorem guarantees the asymptotic validity of the multiplier bootstrap process.

Theorem 5 *Suppose Assumptions (A1)–(A7) hold. Then under either $H_{0,\mathbf{h}}$ or $H_{1n,\mathbf{h}}$,*

$$T_{n,\mathbf{h}}^* \overset{\mathcal{L}^*}{\rightsquigarrow} \mathcal{G} \text{ in probability},$$

where $\mathcal{G}$ is the Gaussian process defined in Theorem 2. Moreover, under $H_{1,\mathbf{h}}$, $T_{n,\mathbf{h}}^*$ weakly converges to a Gaussian process in probability with a distribution different from $\mathcal{G}$.

4 IMPLEMENTATION

Construction of the test process Equation 3 involves the kernel function $K(\cdot)$ and the bandwidth a. To meet Assumptions (A5) and (A6), we choose $K(\cdot)$ to be the standard normal CDF with the bandwidth $a = cn^{-1/3}$, where c is a tuning constant. We have found in extensive simulations that $c = 1/30$ works quite well and is what we recommend in practice, see Web Appendix C.1 in Supplementary Materials for more details.

The projection direction $\mathbf{h}$ is crucial in testing H_0 because it may have a strong impact on the outcome. Although our testing procedure is theoretically consistent, there exist 2 main drawbacks pointed out by Cuesta-Albertos and Febrero-Bande (2010). One is the power loss owing to the projection when transforming a $\mathcal{H}$-valued r.v. into a $\mathbb{R}$-valued r.v.. An extreme case is if one chooses a direction that is orthogonal to the data, that is, $\mathbf{X}^{\mathbf{h}} = 0$, then the P-value of $H_0^{\mathbf{h}}$ is always 1, thus failing to calibrate the level of the test. Moreover, the instability that one may draw the opposite inference from 2 different projected hypotheses remains inevitable.

To alleviate the above issues, we propose to randomly choose *n.proj* > 1 directions, then test the *n.proj* projected hypotheses $\left\{H_{0,\mathbf{h}_j}\right\}_{j=1}^{n.proj}$ simultaneously. We choose to control the FDR instead of employing Bonferroni's method to achieve better power performance. And the selection of projections number *n.proj* is explored in all sorts of different scenarios in the simulation study.

Specifically, we generate the projection direction $\mathbf{h}$ via a data-driven approach, which takes into account of the functional principal component analysis (FPCA) of $\mathbf{X}$ and allows the selection of several different projection directions. FPCA of the functional covariate $\mathbf{X}$ refers to its well-known Karhunen–Loéve expansion:

$$\mathbf{X} = \sum_{j=1}^{\infty} \lambda_j^{1/2} \xi_j \mathbf{e}_j,$$

where eigenvalues $\{\lambda_j\}_{j=1}^{\infty}$ is a decreasing non-negative series, $\{\mathbf{e}_j\}_{j=1}^{\infty}$ is a sequence of orthonormal eigenfunctions of $\mathcal{H}$. The rescaled eigenfunctions $\{\phi_j\}_{j=1}^{\infty}$ are called functional principal components (FPC) of $\mathbf{X}$, $\phi_j = \lambda_j^{1/2}\mathbf{e}_j$, and $\{\xi_j\}_{j=1}^{\infty}$, called FPC scores, are uncorrelated random variables with mean 0 and variance 1.

The projection direction $\mathbf{h}$ is generated from the following procedure.

(i) Compute the eigenvalues $\{\widehat{\lambda}_j\}_{j=1}^{n}$ and eigenfunctions $\{\widehat{\mathbf{e}}_j\}_{j=1}^{n}$ of $\mathbf{X}_1, \ldots, \mathbf{X}_n$ through FPCA.

(ii) Determine the truncated number j_n by

$$j_n = \min\left\{k = 1, \ldots, n-1 : \left(\sum_{j=1}^{k} \widehat{\lambda}_j^2\right) \Big/ \left(\sum_{j=1}^{n-1} \widehat{\lambda}_j^2\right) \leq 0.95\right\}.$$

(iii) Generate the data-driven projection direction $\mathbf{h} = \sum_{j=1}^{j_n} \eta_j \widehat{\mathbf{e}}_j$, where $\eta_j \sim N(0, s_j^2)$ with s_j^2 the sample variance of the jth FPC score.

Repeat the above procedure for *n.proj* times and we get a number of *n.proj* projection directions. For each direction $\mathbf{h}$, the P-value of $H_0^{\mathbf{h}}$ is approximated through the multiplier bootstrap method. Precisely, generate a number of B multiplier bootstrap samples $\left\{T_{n,\mathbf{h}}^{*,b}\right\}_{b=1}^{B}$ in Equation 11, and compute its corresponding testing statistics $\left\{CvM_n^{*b}\right\}_{b=1}^{B}$ as Equation 4. The P-value of $H_0^{\mathbf{h}}$ is $B^{-1}\sum_{b=1}^{B} I\left(CvM_n \leq CvM_n^{*b}\right)$.

After obtaining a number *n.proj* of different P-values, we use the FDR method to mix the resulting P-values. The final P-value is determined as $\min_{i=1,\ldots,n.proj} n.proj \times p_{(i)}/i$, where $p_{(1)} \leq \cdots \leq p_{(n.proj)}$. The following proposition guarantees the consistency of the final P-value for the *n.proj* projected multiple tests regardless of the null hypothesis.

Proposition 4.1 *Denote ordered P-values as* $p_{(1)} \leq \cdots \leq p_{(n.proj)}$ *and let* $\alpha \in (0, 1)$ *be the level of the test, then*

$$\mathbb{P}\left\{\min_{i=1,\ldots,n.proj} \frac{n.proj}{i} p_{(i)} \leq \alpha\right\} \leq \alpha.$$

5 NUMERICAL EVIDENCE

In this section, we examine the finite sample performance of our proposed method. The size and power of the test are examined through the following 4 cases. Throughout this section, we let $\mathcal{H} = \mathcal{L}^2[0, 1]$ be the Hilbert space of all square-integrable functions defined on $[0, 1]$, with the inner product $\langle \mathbf{X}_1, \mathbf{X}_2\rangle = \int_0^1 \mathbf{X}_1(t)\mathbf{X}_2(t)dt$ for $\mathbf{X}_1, \mathbf{X}_2 \in \mathcal{L}^2[0, 1]$.

Case 1: The response variable Y and the functional covariate $\mathbf{X}$ obey the following functional linear model:

$$\begin{aligned} Y_i &= \langle \mathbf{X}_i, \beta\rangle + \epsilon_i, \quad i = 1, \cdots, n; \quad \mathbf{X}_i(t) \\ &= \sum_{j=1}^{100} j^{-(1.1)/2} X_{ij}\phi_j(t), \quad t \in [0, 1], \end{aligned}$$

where X_{ij} and ϵ_i are independent standard Gaussian, $\phi_1(t) = 1$, $\phi_j(t) = \sqrt{2}\cos\{(j-1)\pi t\}$ for $j \geq 2$. Denote $\tilde{\boldsymbol{\beta}} = \left(\tilde{\beta}_1, \cdots, \tilde{\beta}_{100}\right)^{\top}$ with $\tilde{\beta}_1 = 0.3$ and $\tilde{\beta}_j = 4(-1)^j/j^2$ for $j \geq 2$. Let $\beta_j = r\tilde{\beta}_j / \left\|\tilde{\boldsymbol{\beta}}\right\|$ and $\beta(t) = \sum_{i=1}^{100} \beta_j\phi_j(t)$. Here, r^2 corresponds to the strength of the signal and we consider $r^2 = 0, 0.1, 0.2, 0.5$.

Case 2: Y depends on $\mathbf{X}$ in a very non-linear fashion. Let

$$Y_i = r\left\|\mathbf{X}_i\right\|^2 + \epsilon_i, \quad i = 1, \cdots, n,$$

where $\mathbf{X}_i$ and ϵ_i are defined as in Case 1 and $r = 0, 1, 2, 4$.

Case 3: Y depends on $\mathbf{X}$ in another non-linear form. Let

$$Y_i = r\langle e^{-\mathbf{X}_i}, \mathbf{X}_i^2\rangle + \epsilon_i, \quad i = 1, \cdots, n,$$

where $\{\epsilon_i\}_{i=1}^n$ is independent standard Gaussian. The covariates $\{\mathbf{X}_i\}_{i=1}^n$, independent with $\{\epsilon_i\}_{i=1}^n$, are from the Ornstein–Uhlenbeck process, which refers to a Gaussian process with mean function $\mathbb{E}X_t = x_0e^{-\theta t} + \mu\left(1 - e^{-\theta t}\right)$ and covariance function $\mathrm{Cov}\{\mathbf{X}(s), \mathbf{X}(t)\} = (2\theta)^{-1}\sigma^2(e^{-\theta|t-s|} - e^{-\theta|t+s|})$. In this case, we set $\theta = 1/3$, $\sigma = 1$, and $x_0 = 0$. The coefficient r is taken to be 0, 1/20, 1/10, and 1/5, respectively.

Case 4: The data are generated from a simple model with heteroscedasticity. Let

$$Y_i = \left(1 + r\left\|\mathbf{X}_i\right\|^2\right)\epsilon_i, \quad i = 1, \cdots, n,$$

where $\mathbf{X}_i$ and ϵ_i are the same as Case 3, while $r = 0, 0.5, 1, 2$, respectively. It is worth noting that in this case, the conditional mean of Y is independent of $\mathbf{X}$, but the conditional variance is not. Therefore, the classic mean-based tests are unable to detect such independence, while our test still works.

5.1 Dependence on the number of projections

First, we investigate the adequacy of the tests with respect to the number of projections *n.proj*, ranging from 1 to 15. To this end, empirical sizes and powers of the above 4 cases are examined at significance level $\alpha = 0.05, 0.10$. The sample size n is taken to be 50, 100, and 200. Throughout this section, the number of Monte Carlo experiments is set to be $M = 500$ with $B = 2000$ multiplier bootstrap samples in each experiment. We consider a subinterval of quantiles given by $\mathcal{A} = [0.1, 0.9]$, and compute the test-

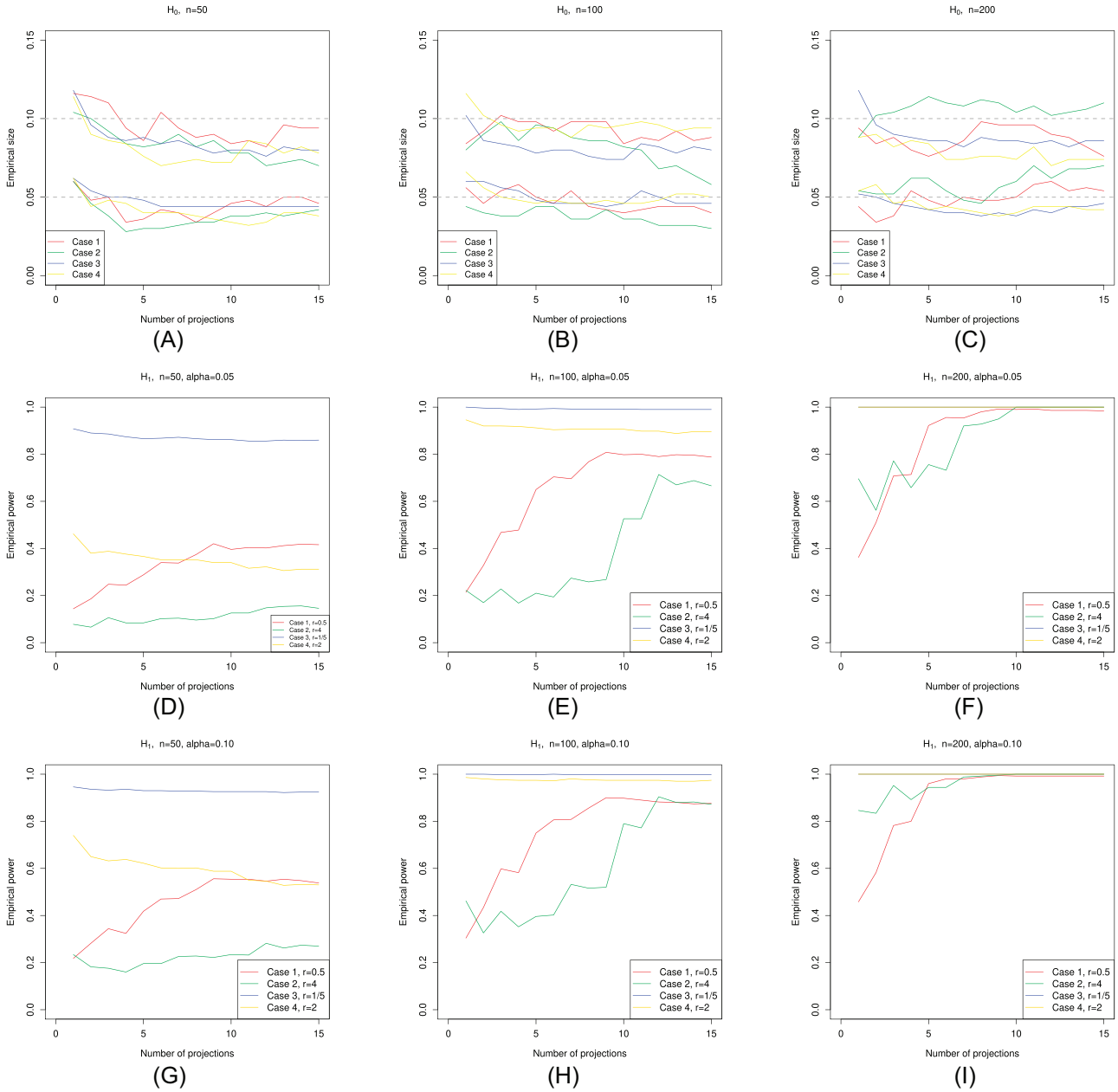

FIGURE 1 Empirical sizes ((A)–(C)) and powers ((D)–(I)) of the test with the number of projections from 1 to 15 in Cases 1-4, based on the sample size $n = 50, 100, 200$ and significance levels $\alpha = 0.05, 0.10$.

ing statistic CvM_n defined in Equation 4 with a grid of $m = 17$ equally spaced points $\{\alpha_j\}_{j=1}^{m}$ in the interval $[0.1, 0.9]$ and $0.1 = \alpha_1 < \cdots < \alpha_m = 0.9$.

Figure 1 (a)–(c) report the empirical sizes of the test under the null hypothesis. It is shown that the small number of projections have an obvious over-rejection of the test, such as Case 3 with $n = 200$ and $\alpha = 0.10$. As the number of projections increase, the empirical rejection rates exhibit mild decrements and stabilize around the nominal level. Figure 1 (d)–(i) display the empirical powers for each case. We can see that certain bumps always exist at the small number of projections, such as in Cases 1 and 2. After that, the power is almost constant for the larger number of projections. Combining the above facts, we tend to choose a moderate number, such as $n.proj = 7, 8, 9$, which not only achieves a perfect balance between the size and power performance but also avoids the heavy computational burden brought by a large number of projections.

5.2 Size and power analysis

Table 1 documents the empirical sizes and powers of the test based on $T_{n,\mathbf{h}}$ in Equation 3 from Cases 1 to 4 with the number of projections $n.proj = 8$ and the quantile interval $\mathcal{A} = [0.1, 0.9]$ at significance level $\alpha = 0.05$. It is shown that the proposed test provides accurate empirical sizes in all cases at both nominal levels, which demonstrates that the multiplier bootstrap works well in approximating the finite sample distribution of the test statis-

TABLE 1 Empirical sizes and powers based on $T_{n,\mathbf{h}}$ under quantile interval $\mathcal{A} = [0.1, 0.9]$ in Casess 1-4, with $\alpha = 0.05$, sample sizes $n = 50$, 100, 200, and 8 projections.

		$n = 50$	$n = 100$	$n = 200$
Case 1	$r^2 = 0$	0.034	0.044	0.048
	$r^2 = 0.1$	0.080	0.178	0.402
	$r^2 = 0.2$	0.116	0.316	0.706
	$r^2 = 0.5$	0.374	0.768	0.980
Case 2	$r = 0$	0.034	0.036	0.046
	$r = 1$	0.070	0.150	0.584
	$r = 2$	0.108	0.254	0.878
	$r = 4$	0.096	0.258	0.928
Case 3	$r = 0$	0.044	0.046	0.038
	$r = 1/20$	0.322	0.610	0.928
	$r = 1/10$	0.610	0.910	1.000
	$r = 1/5$	0.866	0.992	1.000
Case 4	$r = 0$	0.038	0.046	0.040
	$r = 0.5$	0.164	0.610	0.972
	$r = 1$	0.266	0.798	0.996
	$r = 2$	0.352	0.906	1.000

tic under the null. Moreover, the empirical sizes become closer to the nominal significance level as the sample size n increases, providing a positive confirmation of Theorem 2 and Corollary 2. In terms of power, as the deviation coefficient r increases or the sample size n increases, the empirical power increases in all cases. The empirical sizes and powers of the tests based on $T_{n,\mathbf{h}}$ in Equation 3 and $T^{\#}_{n,\mathbf{h}}$ in Equation 6 in Cases 1 to 4 with the significance level $\alpha = 0.10$, and other numbers of projections, such as *n.proj* = 7, 9, are satisfactory across the board, please refer to Table 1 in Supplementary Materials for more details. Performance on power against the local alternatives is displayed in Web Appendix C.4 in Supplementary Materials. Additional simulation results, including size and power analysis with 1 projection, can be found in Web Appendix C.5. We also compare our method with the adjusted Wald test proposed in Li et al. (2022). Results shown in Web Appendix C.6 demonstrate the satisfactory performance of our method and its superiority over that of the adjusted Wald test.

One appealing feature of our test is its capability to measure independence at different quantile levels. Instead of the wide interval [0.1,0.9], we set 3 narrower intervals [0.1,0.3], [0.4,0.6], and [0.7,0.9], representing the independence over low, moderate, and high quantile levels, respectively. Under the above setting, the testing statistic CvM_n defined in Equation 4 is computed with a grid of $m = 11$ equally spaced points $\{\alpha_j\}_{j=1}^{m}$ in $\mathcal{A}$. Table 2 shows the empirical sizes and powers of Case 1 under 3 quantile intervals at significance level 0.05. We can see that empirical sizes are respected under the null hypothesis. But the empirical powers under all 3 quantile intervals are always lower than the counterpart under the quantile interval [0.1,0.9], with a difference 10% − 20%. The reason for power loss is straightforward, independence under a certain interval is the sufficient but not necessary condition for independence under its subinterval. The results of the other 3 cases are quite similar, thus omitted for saving space.

TABLE 2 Empirical sizes and powers based on $T_{n,\mathbf{h}}$ under different quantile intervals $\mathcal{A}$ in Case 1 and Case 5, with $\alpha = 0.05$, sample sizes $n = 50$, 100, 200, and 8 projections.

	$\mathcal{A}$		$n = 50$	$n = 100$	$n = 200$
Case 1	[0.1,0.3]	$r^2 = 0$	0.038	0.062	0.044
		$r^2 = 0.1$	0.086	0.132	0.268
		$r^2 = 0.2$	0.074	0.228	0.480
		$r^2 = 0.5$	0.190	0.504	0.874
	[0.4,0.6]	$r^2 = 0$	0.042	0.052	0.054
		$r^2 = 0.1$	0.100	0.156	0.308
		$r^2 = 0.2$	0.136	0.294	0.604
		$r^2 = 0.5$	0.318	0.606	0.922
	[0.7,0.9]	$r^2 = 0$	0.034	0.052	0.038
		$r^2 = 0.1$	0.060	0.118	0.250
		$r^2 = 0.2$	0.108	0.244	0.492
		$r^2 = 0.5$	0.206	0.516	0.874
Case 5	[0.1,0.3]	$r = 0$	0.050	0.050	0.042
		$r = 1/40$	0.056	0.060	0.074
		$r = 1/20$	0.034	0.062	0.056
		$r = 1/10$	0.042	0.062	0.064
	[0.4,0.6]	$r = 0$	0.060	0.068	0.068
		$r = 1/40$	0.132	0.268	0.486
		$r = 1/20$	0.144	0.276	0.528
		$r = 1/10$	0.150	0.290	0.574
	[0.7,0.9]	$r = 0$	0.038	0.060	0.052
		$r = 1/40$	0.370	0.838	0.998
		$r = 1/20$	0.436	0.896	0.998
		$r = 1/10$	0.446	0.904	1.000

Following the suggestion of the associate editor, we also consider the case in which Y and $\mathbf{X}$ are quantile independent at some quantile levels.

Case 5: The data are generated from the following model with heteroscedastic on τ. Let

$$Y_i = U_i + rI(\tau > 0.5)\langle e^{-\mathbf{X}_i}, \mathbf{X}_i^2\rangle, \quad i = 1, \cdots, n,$$

where $\{U_i\}_{i=1}^{n}$ are i.i.d. random variables with uniform distribution on [0,1], and independent with $\mathbf{X}_i$. The functional covariate $\mathbf{X}_i$ is the same as in Case 3. This leads to a quantile regression model

$$Q_{Y_i|\mathbf{X}_i}(\tau) = \tau + rI(\tau > 0.5)\langle e^{-\mathbf{X}_i}, \mathbf{X}_i^2\rangle,$$
$$i = 1, \cdots, n;\ \tau \in (0, 1).$$

The coefficient r is taken to be 0, 1/40, 1/20, and 1/10, respectively. It is clear that in this case, for the alternative hypotheses with $r > 0$, Y and $\mathbf{X}$ are quantile independent at quantile levels $\tau \in (0, 0.5)$, while quantile dependent at $\tau \in (0.5, 1)$.

We check the empirical sizes and powers of Case 5 under 3 quantile intervals at significance level 0.05, with results shown in Table 2. It is found that empirical rejection rates of the tests under the quantile interval [0.1,0.3] are always close to the significance level regardless of the coefficient r, since Y and $\mathbf{X}_i$ are quantile independent at quantile interval [0.1,0.3]. Both the tests under the quantile interval [0.4,0.6] and [0.7,0.9] exhibit accurate empirical sizes under the null hypothesis. The empirical powers under the quantile interval [0.7,0.9] are always higher than the counterpart under the quantile interval [0.4,0.6], which is not surprising, as Y and $\mathbf{X}_i$ are dependent at the whole quantile interval [0.7,0.9] while partially dependent at the quantile

TABLE 3 The *P*-value of test statistic under the EEG data set based on $T_{n,\mathbf{h}}$(the first row) and $T^{\#}_{n,\mathbf{h}}$(the second row) at different quantile levels with number of projections $n.proj = 7, 8, 9$, respectively.

$\mathcal{A}$	[0.1,0.9]	[0.1,0.3]	[0.4,0.6]	[0.7,0.9]
$n.proj = 7$	0.046	0.252	0.040	0.224
	0.038	0.238	0.024	0.211
$n.proj = 8$	0.048	0.288	0.038	0.210
	0.035	0.272	0.022	0.211
$n.proj = 9$	0.049	0.324	0.038	0.236
	0.038	0.306	0.027	0.218

interval [0.4,0.6]. These findings further confirm that our test provides a comprehensive and powerful tool to check the conditional quantile independence with functional covariate. Full results of the empirical sizes and powers based on $T_{n,\mathbf{h}}$ under different quantile intervals $\mathcal{A}$ in Cases 1 and 5 with the number of projections $n.proj = 7, 8, 9$ and significance levels $\alpha = 0.05, 0.10$ can be found in Table 2 in Supplementary Materials.

6 DATA ILLUSTRATION

The proposed test is further illustrated using EEG data collected by the research group of Prof. Ji Linhong at the Tsinghua University Department of Mechanical Engineering. EEG is known to provide rich information about brain function. In the experiment, 142 university students went through a 5-min closed-eye resting state, and EEG signals were recorded from the scalp location based on the international 10/20 system of electrode placement at a sample rate of 1000 Hz. We truncate EEG signals from 5 min to the first 0.3 s due to the signal periodicity, leading to 300 recorded signal values for each individual. Figure 3(a) in Supplementary Materials displays 5 randomly chosen functional observations of the EEG data.

The working memory ability score is measured by the popular N-back test, in which participants were successively shown a stream of English letters (randomly chosen from A to Z) on a screen and then asked to decide whether each letter matched the one appearing N times before. The score is given in terms of accuracy and reaction time, representing the working memory ability well. It is a continuous variable ranging from −45.092 to 16.414. It is worth noting that the N-back task test does not involve EEG and its score is often used as the variable to be predicted with eyes-closed resting-state EEG signals as input variables.

In our paper, we aim to investigate the conditional quantile independence of the working memory ability score Y on EEG signals (functional covariate $\mathbf{X}$). Hence, the null hypothesis is

$$H_0 : \mathbb{P}\left\{Y \le Q_Y(\tau)|\mathbf{X}\right\} = \tau \ \ a.s., \quad \text{for all } \tau \in \mathcal{A}.$$

We compute the testing statistics with $n.proj = 7, 8, 9$ projections, and $B = 2000$ bootstrap replications. Table 3 presents the *P*-values at different quantile levels. We conclude from the table that for the whole quantile interval and the moderate quantile intervals, the null hypothesis should be rejected at level $\alpha = 0.05$, indicating that the EEG contributes significantly to the quantile of the working memory ability. However, for the higher and lower quantile intervals, we retain the null hypothesis, and there is no sufficient evidence that the conditional quantile of the working memory ability is correlated with EEG signals. The above findings corroborate the classic neuroscience theory, demonstrating the versatility of our method.

To further verify the result of the test, we fit the following FLQM for the working memory ability score Y and EEG curve $\mathbf{X}$:

$$Q_Y(\tau) = \int_{\mathcal{T}} \mathbf{X}(t)\beta(t,\tau)dt + \epsilon, \tag{12}$$

where τ is a pre-determined quantile level, $\beta(\cdot, \tau)$ is a slope function and ϵ is the error.

We estimate $\beta(\cdot, \tau)$ as described by Ramsay and Silverman (2005) using FPCA of $\mathbf{X}$. A total of 19 FPC scores are chosen to capture 99% variance explained by the components used to construct the covariance function of $\mathbf{X}$. We set the fixed quantile level from 0.1 to 0.9. The estimates of $\beta(\cdot, \tau)$ at different quantile levels are displayed in Figure 3(b)-(d) in Supplementary Materials. We adopt the measure R proposed in Koenker and Machado (1999) to evaluate the goodness-of-fit of each quantile regression model, which is calculated by 1 minus the ratio between the sum of absolute deviations in the fully parameterized models and the sum of absolute deviations in the null (non-conditional) quantile model. The higher value represents the better fitting. Specifically,

$$R = 1 - \widehat{V}(\tau)/\widetilde{V}(\tau), \tag{13}$$

where $\widehat{V}(\tau) = \min_{\beta(\cdot,\tau)} \sum_{i=1}^{n} \rho_\tau \left\{Y_i - \int_{\mathcal{T}} \mathbf{X}_i(t)\beta(t,\tau)dt\right\}$ and $\widetilde{V}(\tau) = \min_{b\in\mathbb{R}} \sum_{i=1}^{n} \rho_\tau (Y_i - b)$. To generalize the goodness-of-fit measure into the continuous quantile case, we denote the measure R' as

$$R' = 1 - \int_{\mathcal{A}} \widehat{V}(\tau)\, d\tau \Big/ \int_{\mathcal{A}} \widetilde{V}(\tau)\, d\tau. \tag{14}$$

The results of goodness-of-fit evaluating at single quantile are summarized in Table 4. While for continuous quantile intervals [0.1,0.3], [0.4,0.6], and [0.7,0.9], the corresponding goodness-of-fit measure R' values are 0.086, 0.259, and 0.091, respectively. It is easy to find that among all quantile levels, the significant R values correspond to the moderate levels, such as fixed level 0.4, 0.5, and 0.6; or continuous interval [0.4,0.6], implying that FLQM can explain the relationship between the conditional quantile of the working memory ability score with EEG curves to some extent. However, for low and high quantile levels, both goodness-of-fit measures R and R' are rather small, thus FLQM fails to model the data sufficiently. These findings are consistent with the results of the proposed conditional quantile independence test, further confirming our test's high accuracy and broad applicability.

7 CONCLUDING REMARKS

In our paper, we consider testing conditional quantile independence with functional covariate. The testing statistic from the projected residual marked empirical process weakly converges to a Gaussian process at the root-n rate under the null. We also study its asymptotic behavior under the fixed alternative and a series of local alternatives. The calibration for the critical values of the limiting null distribution is implemented by a straightforward

TABLE 4 The goodness-of-fit measure R in Equation 13 under the EEG data set for the functional linear quantile regression model Equation 12 with different quantile levels.

τ	0.1	0.2	0.3	0.4	0.5	0.6	0.7	0.8	0.9
R	0.077	0.070	0.093	0.221	0.287	0.234	0.105	0.072	0.093

multiplier bootstrap procedure. To our best knowledge, this is the first piece of work in the conditional independence test with functional covariate over a continuum of quantiles, which yields an attractive testing statistic, and at meanwhile is free from the ultra-high dimension as well as user-chosen tuning parameters such as bandwidths. Some promising extensions warrant further investigation. One possible direction is to apply our method to the goodness-of-fit test for the FLQM with a continuum of quantiles. It is not trivial due to the gap in handling the parameter estimation effect.

ACKNOWLEDGMENTS

The authors are truly grateful to the Editor, the AE, and one referee for their insightful comments and constructive suggestions that led to significant improvement of the paper.

SUPPLEMENTARY MATERIALS

Supplementary material is available at *Biometrics* online.

Web Appendices, Tables, Figures, and code referenced in Sections 1– 5 are available with this paper at the Biometrics website on Oxford Academic.

FUNDING

This research is supported by the National Natural Science Foundation of China awards 72373007, 72333001, 12171269, 12301366, and 12026242.

CONFLICT OF INTEREST

None declared.

DATA AVAILABILITY

Data supporting the findings in this paper are available from the corresponding author upon reasonable request.

REFERENCES

Benjamini, Y. and Yekutieli, D. (2001). The control of the false discovery rate in multiple testing under dependency. *The Annals of Statistics*, 25, 1165–1188.

Bücher, A. and Kojadinovic, I. (2016). A dependent multiplier bootstrap for the sequential empirical copula process under strong mixing. *Bernoulli*, 22, 927–968.

Cardot, H., Crambes, C. and Sarda, P. (2005). Quantile regression when the covariates are functions. *Journal of Nonparametric Statistics*, 17, 841–856.

Chen, K. and Müller, H. -G. (2012). Conditional quantile analysis when covariates are functions, with application to growth data. *Journal of the Royal Statistical Society: Series B (Statistical Methodology)*, 74, 67–89.

Chen, X. and Zhou, W. -X. (2020). Robust inference via multiplier bootstrap. *The Annals of Statistics*, 48, 1665–1691.

Chernozhukov, V., Chetverikov, D. and Kato, K. (2013). Gaussian approximations and multiplier bootstrap for maxima of sums of high-dimensional random vectors. *The Annals of Statistics*, 41, 2786–2819.

Chowdhury, J. and Chaudhuri, P. (2019). Nonparametric depth and quantile regression for functional data. *Bernoulli*, 25, 395–423.

Cuesta-Albertos, J. and Febrero-Bande, M. (2010). A simple multiway anova for functional data. *Test*, 19, 537–557.

Cuesta-Albertos, J. A., García-Portugués, E., Febrero-Bande, M. and González-Manteiga, W. (2019). Goodness-of-fit tests for the functional linear model based on randomly projected empirical processes. *The Annals of Statistics*, 47, 439–467.

Escanciano, J. C. and Goh, S. -C. (2014). Specification analysis of linear quantile models. *Journal of Econometrics*, 178, 495–507.

Ferraty, F. and Vieu, P. (2006). *Nonparametric Functional Data Analysis: Theory and Practice*. New York: Springer Science and Business Media.

Hsing, T. and Eubank, R. (2015). *Theoretical Foundations of Functional Data Analysis, with an Introduction to Linear Operators*. Chichester: Wiley.

Kato, K. (2012). Estimation in functional linear quantile regression. *The Annals of Statistics*, 40, 3108–3136.

Koenker, R. and Bassett, G. (1978). Regression quantiles. *Econometrica*, 46, 33–50.

Koenker, R. and Machado, J. A. F. (1999). Goodness of fit and related inference processes for quantile regression. *Journal of the American Statistical Association*, 94, 1296–1310.

Lee, C., Zhang, X. and Shao, X. (2020). Testing conditional mean independence for functional data. *Biometrika*, 107, 331–346.

Lemyre, F. C. and Quessy, J. -F. (2017). Multiplier bootstrap methods for conditional distributions. *Statistics and Computing*, 27, 805–821.

Li, M., Wang, K., Maity, A. and Staicu, A. -M. (2022). Inference in functional linear quantile regression. *Journal of Multivariate Analysis*, 190, 104985.

Mammen, E. (1993). Bootstrap and wild bootstrap for high dimensional linear models. *The Annals of Statistics*, 21, 255–285.

Ramsay, J. O. and Silverman, B. W. (2005). *Functional Data Analysis*. New York: Springer.

Sant'Anna, P. H. and Song, X. (2019). Specification tests for the propensity score. *Journal of Econometrics*, 210, 379–404.

Shi, G., Du, J., Sun, Z. and Zhang, Z. (2021). Checking the adequacy of functional linear quantile regression model. *Journal of Statistical Planning and Inference*, 210, 64–75.

Silverman, B. and Ramsay, J. (2002). *Applied Functional Data Analysis: Methods and Case Studies*. New York: Springer.

Vaart, A. v. d. and Wellner, J. A. (1996). *Weak Convergence and Empirical Processes: With Applications to Statistics*. New York: Springer.

Zhang, Y., Wang, C., Wu, F., Huang, K., Yang, L. and Ji, L. (2020). Prediction of working memory ability based on eeg by functional data analysis. *Journal of Neuroscience Methods*, 333, 108552.

Received: September 16, 2023; Revised: March 10, 2024; Accepted: April 25, 2024